

ROBERT KOCH INSTITUT



Originally published as:

**Stock, N.K., Laraway, H., Faye, O., Diallo, M., Niedrig, M., Sall, A.A.**  
**Biological and phylogenetic characteristics of yellow fever virus lineages from west africa**  
**(2013) Journal of Virology, 87 (5), pp. 2895-2907.**

**DOI: 10.1128/JVI.01116-12**

This is an author manuscript.

The definitive version is available at: <http://jvi.asm.org/>

# Biological and Phylogenetic Characteristics of Yellow Fever Virus Lineages from West Africa

Nina K. Stock<sup>a</sup>, Hewád Laraway<sup>a</sup>, Ousmane Faye<sup>b</sup>, Mawlouth Diallo<sup>b</sup>, Matthias Niedrig<sup>a</sup> and Amadou A. Sall<sup>b</sup>

<sup>a</sup>Robert Koch Institute, Centre for Biological Security 1 (ZBS1), Berlin, Germany

<sup>b</sup>Institut Pasteur de Dakar, Dakar, Senegal

*The yellow fever virus (YFV), the first proven human-pathogenic virus, although isolated in 1927, is still a major public health problem, especially in West Africa where it causes outbreaks every year. Nevertheless, little is known about its genetic diversity and evolutionary dynamics, mainly due to a limited number of genomic sequences from wild virus isolates. In this study, we analyzed the phylogenetic relationships of 24 full-length genomes from YFV strains isolated between 1973 and 2005 in a sylvatic context of West Africa, including 14 isolates that had previously not been sequenced. By this, we confirmed genetic variability within one genotype by the identification of various YF lineages circulating in West Africa. Further analyses of the biological properties of these lineages revealed differential growth behavior in human liver and insect cells, correlating with the source of isolation and suggesting host adaptation. For one lineage, repeatedly isolated in a context of vertical transmission, specific characteristics in the growth behavior and unique mutations of the viral genome were observed and deserve further investigation to gain insight into mechanisms involved in YFV emergence and maintenance in nature.*

## Introduction

Yellow fever virus (YFV) is the prototype of the genus *Flavivirus* of the family *Flaviviridae* and causes yellow fever (YF) disease. In human infections, the symptoms range from asymptomatic or mild characteristics to a hemorrhagic syndrome that can potentially lead to a fatal outcome with organ failure. To date, no specific therapy is available for YF, but a vaccine has been used for many years for the prevention and control of epidemics (1, 2). Despite the effectiveness of the live attenuated vaccine YFV-17D, the World Health Organization (WHO) estimates that 200,000 cases and 30,000 deaths occur annually, mostly in Africa (3).

Over the last 30 years, a major increase of YF infections has occurred due to factors such as low vaccination coverage, urbanization, migration of the human population, reinfestation of *Aedes aegypti*, and improved surveillance (4, 5). In 2005, this led to the “YF initiative” supported by the Global Alliance of Vaccine and Immunization (GAVI), focusing on controlling YF by combining preventive or reactive mass vaccination campaigns with routine immunization. This is realized through an expanded program of immunization in an integrated strategy involving reinforced surveillance of YF and adverse events following immunizations (AEFI) and the management of vaccine supply targeting countries at high risk of YF in West Africa.

The yellow fever virus is transmitted to nonhuman primates in the sylvatic cycle by mosquitoes of the genera *Aedes* in Africa and *Haemagogus* in South America. Humans can be infected when they enter areas of endemicity and can then introduce the virus into cities, where it can contribute to the development of epidemics in the presence of the urban vector *Aedes aegypti* (4, 6).

During dry seasons, YFV can survive through vertical transmission from infected female mosquitoes to their eggs, wherein the viral particles are stable for long periods and can be reactivated when the progeny emerges under better conditions (4, 7).

The incidence of yellow fever depends on the circulation of the mosquito vector and is therefore restricted to the tropical regions of Africa and South America. Surprisingly, YF is absent from Asia, although the epidemic vector *Aedes aegypti* is present in these regions. Hypotheses about a lower vector competence of the mosquito strains in Asia or a cross-protective immunity of the population due

to the presence of other flaviviruses have been debated, but a definite explanation could not be found to date (4, 8, 9).

YFV probably originated in Central Africa, spread subsequently to East and West Africa, and was introduced into the Americas with the slave trade between the 16th and 19th centuries (3, 4).

To date, 7 YFV genotypes have been described (3, 4, 10–12), including 2 in South America and 5 in Africa, namely, West Africa genotype I (Nigeria, Cameroon, and Gabon), West Africa genotype II (Senegal, Guinea, Ivory Coast, and Ghana), East and Central African genotype (Sudan, Ethiopia, Central African Republic, and Democratic Republic of Congo), East African genotype (Kenya), and Angola genotype (Angola).

Most of the phylogenetic studies on YFV used partial sequences of the viral genome (3, 11, 13–16), and the number of complete genome sequences is very limited, especially for wild isolates from an African sylvatic context. Therefore, more sampling and full-length genome sequencing of sylvatic strains are needed to extend our knowledge about the molecular evolution of YFV and could possibly identify new genotypes.

The nucleotide variability among the different genotypes ranges from 25 to 30%, whereas sequence homology within one genotype can be very high even if isolations occurred decades apart, suggesting a very slow evolution rate and a genetic stability of the virus (3, 11, 14, 17).

Interestingly, the incidence of YF outbreaks is not uniform within areas of endemicity. Most of the outbreaks take place in West Africa, whereas outbreaks in East Africa are rather uncommon. The reason for this could possibly be found in the genetic variability that, consequently, could affect the virulence of the virus. Indeed, the West African genotype I shows a higher heterogeneity than the West African genotype II or the East/Central African genotype (11) and could point to a stronger evolutionary activity. In addition, the 3'-nontranslated region (3'-NTR) of the YF viral genome, which contains repeated sequences differing among the genotypes by their numbers of iterations, seems to play an important role in the replication of the virus and hence could have a great impact on virulence (16).

Besides the intrinsic properties of the virus, factors such as host adaptation and vector and host behavior (e.g., movement of populations), as well as climatic and ecological factors, can influence the outcome of an infection. These relationships are complex and raise challenges to investigate the epidemiology and mechanisms in YF emergence and maintenance in nature.

A recent study on molecular evolution of YFV, focusing on sylvatic strains in West Africa (15), showed that (i) 6 different lineages could be identified within Senegal, emphasizing the diversity of YFV circulating in the sylvatic context, (ii) one can speculate that forests such as the Kedougou region could play a role of key reservoir of YFV lineages, generating outbreaks from time to time, and (iii) one specific lineage (lineage 3) seems to be associated with vertical transmission of the virus in nature, raising the question of the impact of genetic diversity on the maintenance mechanism of YFV.

In this context, we analyzed the full-length genome sequences of the different lineages circulating in Senegal and West Africa and investigated their biological properties in insect and human liver cells. Using other YFV sequences from GenBank, we performed phylogenetic analyses based on the complete genome of the virus.

## ***Materials and Methods***

**Virus strains.** Virus strains analyzed in this study were provided by the Institut Pasteur de Dakar, WHO Collaborating Center for arboviruses and viral hemorrhagic viruses (CRORA) in Senegal, and the Robert Koch Institute in Germany (Table 1).

**Cell lines.** Two cell lines have been used for virus cultivation and growth kinetics. Ap61 cells (*Aedes pseudocutellaris*) were grown in L15 (Leibovitz) medium (10% fetal calf serum [FCS], 1% penicillin-streptomycin, 1% glutamine, 10% tryptose phosphate, and 0.05% amphotericin B [Fungizone]) and

incubated at 28°C without CO<sub>2</sub>. HepG2 cells (human hepatocellular carcinoma) were grown in RPMI medium (10% FCS, 1% penicillin-streptomycin, and 1% glutamine) at 37°C with the addition of 5% CO<sub>2</sub>.

**Virus cultivation.** All virus stocks used for the kinetic experiments were produced on Ap61 cells. Cells were grown in cell culture flasks (75 cm<sup>2</sup>) until they reached a confluence of approximately 70%. The medium was discarded, and 500 µl filtered sterile virus solution was added to the cells. The flasks were gently agitated every 10 min during incubation to enhance viral infection. After 1 h, 15 ml L15 medium (2% FCS, 5% tryptose phosphate, 1% glutamine, 1% penicillin-streptomycin, and 0.05% amphotericin B) was added, and the infected cells were incubated for 8 days until a cytopathic effect was observable. The status of infection was tested by real-time PCR, immunofluorescence assay (IFA), and plaque assay. Supernatants were frozen at -80°C for further experiments.

**Growth kinetics.** The growth kinetics were performed in 12-well plates using one plate per virus strain and one uninfected plate as a negative control. Each well was seeded with  $2.4 \times 10^5$  cells in a volume of 400 µl of the appropriate medium with 5% FCS and infected with another 400 µl virus solution, resulting in a multiplicity of infection (MOI) of approximately 0.01 (equates to  $2.4 \times 10^3$  PFU/well). After an incubation time of 4 h, the medium was removed and replaced with 2 ml of new medium to set a zero point for the growth curves. The harvesting of one well occurred immediately before and after the change of the infection medium and at 22, 28, 50, 75, 99, 124, and 146 h postinfection. Each harvest was performed as follows. Supernatants were removed and frozen at -80°C in small aliquots. Cells were washed once with phosphate-buffered saline (PBS) and then removed in 500 µl PBS. One drop of this solution was dried on a glass slide for a subsequent immunofluorescence assay. The residual 250 µl of cells was centrifuged for 5 min at maximum speed, resuspended in 350 µl of RLT buffer plus β-mercaptoethanol (RNeasy minikit; Qiagen), and frozen at -80°C for RNA extraction.

**Plaque assay.** To determine the amount of infectious viral particles (PFU),  $6 \times 10^5$  PS cells (porcine kidney epithelial cells) in 200 µl L15 medium (5% FCS, 1% penicillin-streptomycin, and 1% glutamine) were seeded in each well of a 24-well plate. Serial dilutions of the appropriate virus suspension ranging from  $10^{-1}$  to  $10^{-7}$  were added to the wells, also in a volume of 200 µl L15 medium. After an incubation period of approximately 4 h, the cells were covered with 400 µl overlay medium (L15 plus 5% FCS, 1% penicillin-streptomycin, 1% glutamine, and 1.6% carboxymethyl cellulose) and incubated again for 4 (YFV strains 17D and Asibi) or 7 (mosquito isolates) days at 37°C without the addition of CO<sub>2</sub>. Afterwards, the cells were fixed for 15 min with 3.7% formaldehyde and stained for at least 30 min with naphthol black solution (1 g naphthol blue black, 13.6 g sodium acetate, and 60 ml glacial acetic acid per 1 liter H<sub>2</sub>O). Considering the most appropriate viral dilution, infected cells were visible as plaques and calculation of PFU per ml was carried out according to Ferguson and Heath (18).

**Immunofluorescence assay.** Cells were dissolved in PBS and dropped on a glass slide. After complete drying, cells were fixed for at least 10 min in cold acetone, dried again, and then stored at -20°C until staining. Staining was done with a YFV-specific monoclonal mouse anti-E-protein antibody (MAK 6330) (19) diluted 1:100 in PBS and incubated 1 h at 37°C. After washing three times with PBS, cells were incubated with the second antibody (goat anti-mouse IgG, fluorescein isothiocyanate [FITC] conjugated; Dianova), diluted 1:200 in PBS, for 1 h at 37°C in the dark. The cells were washed again three times with PBS, dried, and covered with ProLong Gold antifade reagent with 4',6-diamidino-2-phenylindole (DAPI) (Invitrogen). After dehydration, examination was done by fluorescence microscopy (Biozero microscope; Keyence).

**RNA extraction and real-time PCR.** Extraction of viral RNA from cell culture supernatants was performed with the QIAamp viral RNA minikit (Qiagen) according to manufacturer's instructions. For RNA extraction from the cell fraction, cells were lysed in RLT buffer plus β-mercaptoethanol (RNeasy minikit; Qiagen) and homogenized using the QIAshredder columns from Qiagen. Further purification of the RNA was done according to the protocol of the RNeasy minikit (Qiagen).

For the detection and quantification of viral RNA, a YFV-specific real-time assay was applied as described previously (20).

**Full-length genome sequencing.** For the full-length genome sequencing, viral RNA was extracted from the supernatants of YFV-infected Ap61 cells using the QIAamp viral RNA minikit (Qiagen). cDNA synthesis, PCR, and sequencing were done as described elsewhere (21, 22).

Phylogenetic analyses. The whole genome sequences of 24 YFV strains and one Sepik virus strain (Tables 1 and 2) serving as an outgroup were aligned using the muscle alignment tool implemented in Geneious Pro version 5.4.3 (Biomatters Ltd.).

The phylogenetic analyses were performed with the Bayesian and maximum likelihood (ML) methods. Model selection and the Bayesian analyses were performed as described previously using the programs jModelTest and Mr Bayes 3.1.2 (22, 23). The ML analyses were carried out using the program SeaView version 4.3.5 (<http://pbil.univ-lyon1.fr/software/seaview.html>) (24). For this analysis, a general time-reversible model plus gamma distribution (GTR+G model) was selected according to the jModelTest analysis and further settings were left at default values. This analysis was performed with 1,000 bootstraps. The resulting Bayesian and ML consensus trees were visualized with the software FigTree version 1.3.1 (<http://tree.bio.ed.ac.uk/software/figtree>). Trees were rooted to the outgroup Sepik virus, and to ensure visual clarity, the branches were transformed to a cladogram style.

Nucleotide sequence accession numbers. All full genome sequences generated in this work have been submitted to the GenBank database under accession numbers JX898868 to JX898881.

## Results

Full-length genome sequencing. In this study, 14 YFV isolates were completely sequenced and included 9 representatives of the different lineages (except lineage 2) circulating in the sylvatic context of Kedougou that have already been sequenced partially (15). Furthermore, 5 new YFV strains (6857, 6858, 6865, 6866, and 6867), isolated from mosquitoes during the sylvatic amplification in Kedougou in 2005, have been sequenced completely (Table 1). Overall, full genome sequences could be obtained for all chosen YF strains.

Two positions of nucleotide variants with effects on the protein level could be identified, presumably reflecting heterogeneity in the virus population. The first one is a “Y” at nucleotide position 1140 (E protein, amino acid [aa] 56) of strain 357, leading either to the amino acid alanine or valine. The second is an “R” at nucleotide position 1376 (E protein, aa 135) of strains 6857, 6858, 6865, 6866, and 6867, forming the amino acid isoleucine or valine (Figure 1).

Considering the comparison of the protein sequence throughout the viral open reading frame (ORF), the differences clearly reflect the diverse YF lineages (Figure 1). For lineage 1, only one strain was available for sequencing, and thus it appears here as a single isolate. The strains belonging to lineage 4 (strain 357 compared to the strains isolated in 2005, classified as L4) differ the most among each other by 0.41%, whereas the strains of lineages 5 and 6 show variances of only 0.18% and 0.26%, respectively. Lineage 3 shows 100% identity among the sequenced strains 333 and 335 at the amino acid level. Also, the YFV strains isolated in 2005 in the Kedougou region (6857, 6858, 6865, 6866, and 6867) exhibited the same sequence, even though they were isolated from three different mosquito vectors (Table 1), and were identified as lineage 4 by phylogenetic analyses (Figure 2). Considering only the alignment of the E protein region, we found a variability of 1% for lineage 4, 0.4% for lineage 5, and 0% for lineages 6 and 3.

Compared to the reference strain Asibi, variability among amino acids varies between 0.53% for lineage 4 and 1.08% for lineage 1 (Table 3). However, closer examination of the mutations representing unique features of each lineage (which are defined as the number of mutations that are unique to this lineage/total number of differences in this lineage compared to the Asibi strain) reveals that discrepancies between the lineages are huge. While the amount of unique features ranges from 5.5 to 22% for lineages 4, 5, and 6, lineage 1 exhibits unique characteristics of 56.8% and lineage 3 of 90%. Most of these unique mutations for lineage 3 are located in the E, NS4B, and NS5 proteins (Table 3).

It is noteworthy that strain 307 (lineage 1, Ivory Coast 1973) has an insertion just after the stop codon in the 3'-NTR (nucleotide position 3, counted from the beginning of the stop codon of the viral polyprotein) and a deletion at position 174. The latter mutation was previously described for strain 85-82H, isolated in Ivory Coast in 1982, but the insertion was found at position 304 in this case (25). Apart from the deviating insertion, strain 307 exhibits a similar sequence in the 3'-NTR as strain 85-82H.

The strains of lineage 3 show unique mutations at four positions in the 3'-NTR that distinguish them from the other strains (7, 8, 54, and 449, counted from the beginning of the stop codon of the viral polyprotein). The alignment of the whole 3'-NTR of all sequenced YFV strains is shown in Figure 3.

Phylogeny of YFV isolates from West Africa. A total of 24 YFV full genomes have been used for phylogenetic analyses (Tables 1 and 2). The phylogenetic tree from the ML analysis was consistent with the tree that was obtained by Bayesian analysis regarding its topology. Figure 2 shows the consensus tree of the Bayesian analysis performed with 10 million generations.

The obtained consensus tree basically shows a clustering in the same subgroups as the phylogenetic tree based on E protein sequences (15). The East and Central African genotypes are clearly separated from the West African genotypes (Figure 2). In previous studies, the East and Central African strains Couma, Uganda, and Angola were considered independent genotypes (3, 11, 12) but appear here in one clade. This may be due to the limited numbers of complete genome sequences available for this study.

The West African genotypes show a clustering into the different lineages described previously. One clade represents lineage 1 and is composed of two strains from Ivory Coast. The second clade is composed of the wild-type reference strains Asibi and French viscerotropic virus, isolated for the first time in 1927 from YF patients in West Africa (26). Clade 3 contains the Senegalese lineage 3 and the strain Trinidad79A, representing the only full genome sequence coming from South America. The fourth clade within the West African genotypes represents lineage 4 and contains the newly sequenced YF strains 6857, 6858, 6865, 6866, and 6867. They are identical in their nucleotide sequences and represent only one single virus strain (see above); hence, they appear as a polytomy in our tree. Clade 5 contains the strains belonging to lineage 5 together with a strain from Gambia, and clade 6 represents lineage 6 including another strain isolated in Ivory Coast.

Growth kinetics. In order to investigate whether the diversity of YFV has an impact on its biological properties, growth kinetics of the different lineages were determined in mosquito (Ap61) and human liver cells (HepG2) to reflect the natural hosts (insect vector and primate). Hence, strains 333, 357, 345, 314, and 307 were tested as representatives of the different YF lineages circulating in West Africa (Table 1; lineage 2 was not at our disposal), while the 17D vaccine and the wild-type strain Asibi were used as controls.

The status of infection was visualized by immunofluorescence staining of the cells and quantitative reverse transcriptase PCR (qRT-PCR) of RNA equivalents isolated from supernatants and cells. Additionally, we determined the amount of infectious viral particles (PFU/ml) from the supernatant fraction by plaque assay. The experiments were duplicated in order to confirm the growth behavior of the different virus strains and analyzed regarding genome equivalents in cell supernatants. Range values of these two approaches are depicted in the corresponding data curves in Figure 4 (see also Figure 6 and 7).

In Figure 4, all tested parameters are shown for the strains Asibi, 357 (lineage 4), and 333 (lineage 3). In Figure 4a, the Asibi strain clearly shows better replication in HepG2 cells than in Ap61 cells by reaching titers up to 3 logs higher in a period of 2 to 4 days after infection. Nevertheless, nearly equivalent titers are obtained in both cell lines after 6 days. After 1 week, the growth curves from Ap61 cells are still increasing, whereas growth in HepG2 cells is already decreasing after 100 h. This is consistent with the result of the immunofluorescence assay (IFA), showing cells dying after 99 h in HepG2 cells. Ap61 cells are stable until the end of the experiment when infected with YFV Asibi (Figure 5).

Strain 357 (Figure 4b) shows similar growth in both cell lines, as growth curves are stagnating or decreasing after 100 h. In contrast to the reference strain Asibi, HepG2 cells remain stable throughout the experiment when infected with strain 357, whereas Ap61 cells started dying after 124 h (Figure 5, IFA).

For strain 333 (Figure 4c), we observed significant differences in the growth curves of the two cell lines. In HepG2 cells, the growth of strain 333 is comparable to the YFV reference strains. In Ap61 cells, nearly no replication activity was detectable by PCR or plaque assay. Likewise, no clear infection

was visible by IFA (Table 4), although we could observe the early stages of cell death 24 h after infection.

In terms of growth behavior, the replication rate of all YFV strains in HepG2 cells is comparable regarding the quantity of RNA copies and PFU (Figure 6). Differences are only visible by microscopic observation and IFA. In fact, the reference strains Asibi and 17D, as well as strain 333 (lineage 3), affect the cells after only 4 days of cultivation (Figure 5, shown for YFV Asibi), whereas strains 345, 314, and 307 (lineages 5, 6, and 1) kill the cells more slowly from the beginning of day 5 (data not shown). Strain 357 (lineage 4) had no major effect on the cells throughout the experiment (Figure 5).

The Ap61 cellular environment elucidated more differences between the strains. First, the reference strains Asibi and 17D exhibit the same growth behavior, but their maximum titers during this experiment were lower than those for strains 307, 314, 345, and 357 (Figure 7). Another distinction between the reference strains and the mosquito isolates can be seen in the cell uptake (Figure 7b). Shortly after infection, RNA copies were undetectable in the cell fraction infected with 17D and Asibi, whereas in all other strains, RNA copies were already detectable. The curve progression of the virus titer for the reference strains is still increasing at the end of the experiment, which can also be demonstrated by IFA (Fig. 5, strain Asibi; Table 4), where cells are still in good condition and not yet completely infected after 146 h. The curve progression for the other strains (except strain 333) is either stagnating or regressing. This process is also supported by IFA, where cell death is visible after 124 h for strains 357, 314, and 307 and after only 76 h for strain 345 (Figure 5, strain 357). Strain 333, representing lineage 3, stands out from the other strains regarding the progression of the growth curve. The cell uptake seems to be similar to that of the other mosquito isolates (reflected by intracellular RNA in Figure 7b), but there is no clear increase of the titer showing replication activity in Ap61 cells (Figure 4c and 7). Although we could observe the beginning of cell death 24 h postinfection, the IFA remained negative (Table 4).

Comparing the growth behavior between the two cell lines, strains 307, 357, 345, and 314 (belonging to lineages 1, 4, 5, and 6, respectively) show similar growth curves regarding the number of RNA copies and infectious particles (Figure 6 and 7), but when considering IFA results, Ap61 cells seem to be much more affected than HepG2 cells (Figure 5, strain 357).

The reference strains Asibi and 17D replicate much better and generate higher titers in HepG2 cells and induce cell death in HepG2 cells much faster than in Ap61 cells (Figure 5). Their growth in Ap61 cells is much slower and seems to occur concurrently with a poor uptake in the cells (Figure 7b). Even though 17D is the attenuated vaccine strain of YFV Asibi, and Asibi a wild-type virus, both strains show the same growth progression in these experiments.

Strain 333 (lineage 3) seems not to replicate effectively in Ap61 cells (Figure 4c and 7). In HepG2 cells, this strain shows the same growth curves for RNA copies and infectious viral particles as the other mosquito isolates, but it damages the cells much faster, showing a comparable picture to the one presented by the reference strains.

## **Discussion**

Sequence analysis. Here we provide a total of 14 new full genome sequences from West African YFV isolates, mainly deriving from Senegal. Nine of them were previously sequenced for the E protein-coding region and classified into different lineages (15), whereas 5 isolates were sequenced for the first time in this study and identified as lineage 4, based on the work of Sall et al. (15).

Six of the sequenced strains (357, 6857, 6858, 6865, 6866, and 6867), all belonging to lineage 4, show heterogeneity in their virus population with an effect at the protein level. In all cases, the position is located in the E protein, which is known to be subjected to the highest selection pressure among all viral proteins.

The newly sequenced isolates 6857, 6858, 6865, 6866, and 6867 revealed no differences within their genomes despite the diversity of vector hosts (*Aedes furcifer*, *Aedes taylori*, and *Aedes luteocephalus*), suggesting not only YFV genetic stability but also that one lineage (lineage 4)

emerged in 2005. This lineage reemerges following its appearance from 1976 to 1979 and 2001, reinforcing the hypothesis that the different YFV lineages are enzootic in Kedougou and can emerge together or alternatively within Senegal or in West Africa (15).

On closer examination of the amino acid sequence of the viral polyprotein, the YF isolates can clearly be assigned to the different lineages identified in advance (Figure 1). Regarding the amount of their differences compared to the reference strain Asibi, the strains are quite similar. Most striking is the large quantity of unique features of lineage 1 (strain 307) with 56.8% and lineage 3 (strains 333 and 335) with 90%, quantified in relation to all amino acid differences from Asibi (Table 3).

This divergence is especially marked for lineage 3 in terms of the deviating replication in the growth kinetics compared to the other strains analyzed in this study (see below) (Figure 7). The relevant mutations for lineage 3 accumulate in the proteins E, NS4B, and NS5.

Whereas the E protein is the major envelope protein responsible for cell entry and membrane fusion (27), and thus subject to high selection pressure, NS4 and NS5 are nonstructural proteins functioning as components of the viral replication complex. The function and structure of the flaviviral NS4 protein are not yet fully understood. However, the NS4B subunit, in which lineage 3 shows four unique mutations, is most likely associated with the endoplasmic reticulum (ER) membrane and inhibits the interferon signaling pathway (28, 29).

The structure and function of the flavivirus NS5 protein have further investigated (30, 31). The methyltransferase domain, which is essential for the mRNA capping process, lies in the N-terminal domain of the protein. Here we find two mutations of strain 333 (aa 2 and 258), which are located in the variable regions surrounding the conserved core region of the protein (aa 59 to 224).

The residual C-terminal part of the NS5 protein comprises the RNA-dependent RNA polymerase domain (RdRp), exhibiting the typical finger, palm, and thumb subdomains of a polymerase and which is essential for *de novo* RNA synthesis and hence for viral replication. Within this domain, lineage 3 shows four unique mutations (aa 335, 351, 660, and 878).

Studies on dengue virus show that amino acids 335 and 351 are located within a region interacting with the NS3 protein and importin- $\beta$  and thus functioning as a nuclear localization sequence (31). Even more striking is position 660, which is located within the active site of the palm subdomain, just adjacent to aa663, which has been shown to play a crucial role in the catalytic activity of the protein (31). This leads us to the assumption that these mutations could have an impact on the impaired growth behavior of this YFV strain in Ap61 cells.

The 3'-NTR. The 3'-NTR of flaviviruses is known to develop a secondary structure which is considered to play an important role in viral replication and translation initiation (16, 32, -,34). Domain III, which lies at the very end of the 3'-NTR and forms a secondary structure known as the 3' long stable hairpin (3'-LSH), is believed to build the functional core of the 3'-NTR (33, 34). In contrast, the domains between the stop codon and the 3'-LSH are much more divergent and seem to function as nonessential enhancer elements for replication, especially in the mammalian host (32, 35). Several studies focusing on the variability and the secondary structure of these domains (16, 32, 34) could identify hot spots of nucleotide variation (32) or wild isolates with large deletions or duplications (36) which did not affect the ability of the virus to replicate. Differences in pathogenicity between vaccine and wild-type strains could be traced back to an alternative folding of the 3'-LSH in domain III (33).

Strain 307 (lineage 1) shows two exceptional mutations in the 3'-NTR compared to the other West African strains (Figure 3). One is an insertion just after the stop codon and the other is a deletion of 170 bases farther downstream. Similar mutations have already been found in a strain also isolated in Ivory Coast, in relation to an outbreak in 1982 (25). As the secondary structure of this strain has already been elucidated and the unique deletion in strain 307 at position 3 lies in an area described as a hot spot of nucleotide variation (32), these mutations may not affect the secondary structure and the function of the 3'-NTR.

The same applies for the mutations in the 3'-NTR observed for lineage 3. The mutations occur either in a hot spot of nucleotide variation (nucleotides 7 and 8), in the F3 loop of repeated sequence 1 (RYF1) (nucleotide 54), which is known to be nonessential for viral replication, or in the Lsh3 region of

the 3'-LSH (nucleotide 449). The latter region lies within the functional core for viral replication but is known to accumulate mutations without an effect on stem formation (32).

**Phylogenetic analysis.** The phylogenetic analyses, based on the full genome nucleotide sequences performed in this study, revealed a similar tree topology compared to the analyses based on E protein sequences for the West African YF strains (15). However, due to a restricted number of YFV isolates and full genome sequences, the possibilities to investigate the diversity and evolution of YFV in this study remain limited. Limitation is evident considering the subgroup of East and Central African genotypes of the Bayesian tree (Figure 2), where the YFV strains that have clearly been classified as independent genotypes in various studies (3, 11) appear here in a single clade. Further sampling and sequencing especially of East and Central African YFV wild isolates are necessary for a detailed division and could even uncover the existence of additional lineages, as shown here for the West African clade.

In addition, monitoring of YFV distribution and evolution could strongly contribute to the understanding of the development of outbreaks and the complexity of viral zoonoses in general.

The YF strain Trinidad79A is the only South America strain included in our phylogenetic analyses and is closely related to the Senegalese YF lineage 3. Previous studies by Chang et al. (13) on E protein sequences already suggested that this strain was a recent introduction from West Africa to Trinidad. In contrast, Wang et al. (16) classified this strain as derived from a South American genotype in their analyses of the 5'-NTR, the NS4 protein, and the 3'-NTR. Full genome sequencing of additional South American strains is needed to answer the question about the origin of the Trinidad79A strain.

Two separate YF lineages are present in Ivory Coast, one clustering with the Senegalese lineage 6 and the other one with lineage 1. This classification reflects a cocirculation of two different genotypes in Ivory Coast (West African genotypes I and II) or, due to the temporal separation of the isolations in 1982 and 1999 (25, 37), a switch in circulation from West African genotype I to West African genotype II.

**Growth kinetics.** To investigate the growth behavior of the different YF lineages circulating in Senegal, we performed growth kinetics on cells from the mosquito vector (Ap61) and human liver cells (HepG2). HepG2 cells have been used in several studies to investigate viral infections, especially of flaviviruses, and were thus chosen as the model cell line for our examinations (38,–,41). The aim of this experimental setup with the two cell lines was to cover the natural system of both the transmitting vector and the vertebrate host. We used the well-known prototype strain Asibi and the vaccine strain 17D as reference strains.

In human liver cells, the replication rates of the virus were similar for all strains. Differences were only revealed by microscopical observation, showing that the reference strains 17D and Asibi and isolate 333 (lineage 3) are affecting the cells earlier than the other strains that were isolated from mosquitoes.

Studies that compared the growth behavior of 17D and Asibi in HepG2 cells showed a higher susceptibility of the cells for the attenuated virus strain 17D within the first 3 days after infection (38). We also observed by IFA a lower infectivity of HepG2 cells with Asibi than that with 17D within 50 h postinfection. Nevertheless, the cells showed complete infection after 75 h for both strains (Table 4). In Ap61 cells, the contrary effect was observed by IFA, resulting in a lower infection of the cells with the strain 17D. All further analyzed parameters showed no difference in growth behavior between 17D and Asibi (Fig. 6 and 7).

In insect cells, 17D and Asibi replicate much slower than the mosquito derived isolates (with the exception of strain 333), which probably could be explained by a poor uptake in the cells (Figure 7).

The strain Asibi was isolated from a YF patient, and 17D arose from it through serial passaging (26). Both strains have been in laboratory use since their isolation in 1927 and the detailed passage history of many laboratory strains in use today is not always clear. Unlike these human isolates, all the other strains examined here originated from mosquitoes and have just a brief passage history mostly on insect cells. Hence, a previous adaptation to the appropriate host could be a possible explanation for the differential cellular damage of these strains in the insect and human cells in our study.

In nature, YFV always switches between insect vector and primate without apparent adaptation to one of these hosts and the genetic stability of the virus has consistently been confirmed by many studies (3, 11, 14, 17).

A study by Cooper and Scott (42) demonstrates that these ideas do not necessarily have to be contradictory. They could show that strains of eastern equine encephalitis virus (EEEV), which have been cultivated by alternating passaging between insect and avian cells, exhibited a higher virion production in both cell lines than strains that have been cultivated in only one cell type. Furthermore, EEEV strains that have been adapted to insect cells showed an increased susceptibility to insect cells, whereas strains adapted to avian cells showed unimproved growth in both cell lines. These results indicated that alternating hosts select for virus populations that are able to replicate well in both systems.

In both cell lines, strain 333 (lineage 3) presented distinctive behavior. In human liver cells, it is surprising that the growth of strain 333 more closely resembles that of the reference strains isolated from YF patients than that of the other mosquito isolates.

Moreover, this lineage is the only one that could be linked with vertical transmission in nature until now (15). Also in this case, strain 333 was isolated from a male mosquito or a female neonate, thus arising from vertical transmission. In our study, this strain did not replicate efficiently in Ap61 cells (Figure 4c and 7), which are derived from *Aedes pseudoscutellaris* larvae. Vertical transmission and persistence in mosquito eggs is a mechanism of long-time survival or rather a maintenance mechanism of the virus. At this stage, only minimal cell metabolism is detectable in insect cells. Our experiments did not show clear replication activity by plaque assay, PCR, or IFA, but we observed early cellular damage due to virus infection. As viral replication relies on the replication machinery of the host cell, early cellular damage probably caused the stagnating growth curve observed in our analysis. How this coincides with the adaptation of the virus to mosquito cells or with the maintenance mechanism of vertical transmission remains to be elucidated.

Taking these observations into account, together with the sequence differences in the viral polyprotein compared to all the other strains, a further analysis of this lineage would be very interesting for the investigation of certain protein functions and for the understanding of vertical transmission.

## ***Acknowledgments***

Cells were kindly provided by Sonja Linke (Ap61) and Anke Walther (HepG2) from the Centre for Biological Security 1 at the Robert Koch Institute in Berlin, Germany. In addition, we cordially thank the sequence laboratory at the Robert Koch Institute for assistance and Camille Escadafal, Marc Appelhans, and Amy Mikhail for correction of the manuscript.

## References

1. Monath TP. 2008. Treatment of yellow fever. *Antiviral Res.* 78:116–124.
2. Monath TP. 2001. Yellow fever: an update. *Lancet Infect. Dis.* 1:11–20.
3. Mutebi JP, Barrett AD. 2002. The epidemiology of yellow fever in Africa. *Microbes Infect.* 4:1459–1468.
4. Barrett AD, Monath TP. 2003. Epidemiology and ecology of yellow fever virus. *Adv. Virus Res.* 61:291–315.
5. Robertson SE, Hull BP, Tomori O, Bele O, LeDuc JW, Esteves K. 1996. Yellow fever: a decade of reemergence. *JAMA* 276:1157–1162.
6. Gould EA, Solomon T. 2008. Pathogenic flaviviruses. *Lancet* 371:500–509.
7. Fontenille D, Diallo M, Mondo M, Ndiaye M, Thonnon J. 1997. First evidence of natural vertical transmission of yellow fever virus in *Aedes aegypti*, its epidemic vector. *Trans. R. Soc. Trop. Med. Hyg.* 91:533–535.
8. Barrett AD, Higgs S. 2007. Yellow fever: a disease that has yet to be conquered. *Annu. Rev. Entomol.* 52:209–229.
9. Gould EA, de Lamballerie X, Zanotto PM, Holmes EC. 2003. Origins, evolution, and vector/host coadaptations within the genus *Flavivirus*. *Adv. Virus Res.* 59:277–314.
10. de Souza RP, Foster PG, Sallum MA, Coimbra TL, Maeda AY, Silveira VR, Moreno ES, da Silva FG, Rocco IM, Ferreira IB, Suzuki A, Oshiro FM, Petrella SM, Pereira LE, Katz G, Tengan CH, Siciliano MM, Dos Santos CL. 2010. Detection of a new yellow fever virus lineage within the South American genotype I in Brazil. *J. Med. Virol.* 82:175–185.
11. Mutebi JP, Wang H, Li L, Bryant JE, Barrett AD. 2001. Phylogenetic and evolutionary relationships among yellow fever virus isolates in Africa. *J. Virol.* 75:6999–7008.
12. von Lindern JJ, Aroner S, Barrett ND, Wicker JA, Davis CT, Barrett AD. 2006. Genome analysis and phylogenetic relationships between east, central and west African isolates of Yellow fever virus. *J. Gen. Virol.* 87: 895–907.
13. Chang GJ, Cropp BC, Kinney RM, Trent DW, Gubler DJ. 1995. Nucleotide sequence variation of the envelope protein gene identifies two distinct genotypes of yellow fever virus. *J. Virol.* 69:5773–5780.
14. Lepiniec L, Dalgarno L, Huong VT, Monath TP, Digoutte JP, Deubel V. 1994. Geographic distribution and evolution of yellow fever viruses based on direct sequencing of genomic cDNA fragments. *J. Gen. Virol.* 75(Pt 2):417–423.
15. Sall AA, Faye O, Diallo M, Firth C, Kitchen A, Holmes EC. 2010. Yellow fever virus exhibits slower evolutionary dynamics than dengue virus. *J. Virol.* 84:765–772.
16. Wang E, Weaver SC, Shope RE, Tesh RB, Watts DM, Barrett AD. 1996. Genetic variation in yellow fever virus: duplication in the 3' noncoding region of strains from Africa. *Virology* 225:274–281.
17. Deubel V, Pailliez JP, Cornet M, Schlesinger JJ, Diop M, Diop A, Digoutte JP, Girard M. 1985. Homogeneity among Senegalese strains of yellow fever virus. *Am. J. Trop. Med. Hyg.* 34:976–983.
18. Ferguson M, Heath A. 2004. Collaborative study to assess the suitability of a candidate International Standard for yellow fever vaccine. *Biologicals* 32:195–205.
19. Gelderblom HR, Kocks C, L'Age-Stehr J, Reupke H. 1985. Comparative immunoelectron microscopy with monoclonal antibodies on yellow fever virus-infected cells: pre-embedding labelling versus immunocyoultramicrotomy. *J. Virol. Methods* 10:225–239.
20. Weidmann M, Faye O, Kranaster R, Marx A, Nunes MR, Vasconcelos PF, Hufert FT, Sall AA. 2010. Improved LNA probe-based assay for the detection of African and South American yellow fever virus strains. *J. Clin. Virol.* 48:187–192.
21. Bae H-G. 2006. Analyse der Immunantwort nach Infektion mit Gelbfiebertviren. Freie Universität Berlin, Berlin, Germany.
22. Stock NK, Boschetti N, Herzog C, Appelhans MS, Niedrig M. 2012. The phylogeny of yellow fever virus 17D vaccines. *Vaccine* 30:989–994.
23. Ronquist F, Huelsenbeck JP. 2003. MrBayes 3: Bayesian phylogenetic inference under mixed models. *Bioinformatics* 19:1572–1574.
24. Gouy M, Guindon S, Gascuel O. 2010. SeaView version 4: a multiplatform graphical user interface for sequence alignment and phylogenetic tree building. *Mol. Biol. Evol.* 27:221–224.
25. Pisano MR, Nicoli J, Tolou H. 1997. Homogeneity of yellow fever virus strains isolated during an epidemic and a post-epidemic period in West Africa. *Virus Genes* 14:225–234.
26. Frierson JG. 2010. The yellow fever vaccine: a history. *Yale J. Biol. Med.* 83:77–85.
27. Mukhopadhyay S, Kuhn RJ, Rossmann MG. 2005. A structural perspective of the flavivirus life cycle. *Nat. Rev. Microbiol.* 3:13–22.

28. Miller S, Kastner S, Krijnse-Locker J, Buhler S, Bartenschlager R. 2007. The non-structural protein 4A of dengue virus is an integral membrane protein inducing membrane alterations in a 2K-regulated manner. *J. Biol. Chem.* 282:8873– 8882.
29. Munoz-Jordan JL, Sanchez-Burgos GG, Laurent-Rolle M, Garcia-Sastre A. 2003. Inhibition of interferon signaling by dengue virus. *Proc. Natl. Acad. Sci. U. S. A.* 100:14333–14338.
30. Bollati M, Alvarez K, Assenberg R, Baronti C, Canard B, Cook S, Coutard B, Decroly E, de Lamballerie X, Gould EA, Grard G, Grimes JM, Hilgenfeld R, Jansson AM, Malet H, Mancini EJ, Mastrangelo E, Mattevi A, Milani M, Moureau G, Neyts J, Owens RJ, Ren J, Selisko B, Speroni S, Steuber H, Stuart DI, Unge T, Bolognesi M. 2010. Structure and functionality in flavivirus NS-proteins: perspectives for drug design. *Antiviral Res.* 87:125–148.
31. Malet H, Masse N, Selisko B, Romette JL, Alvarez K, Guillemot JC, Tolou H, Yap TL, Vasudevan S, Lescar J, Canard B. 2008. The flavivirus polymerase as a target for drug discovery. *Antiviral Res.* 80:23–35.
32. Mutebi JP, Rijnbrand RC, Wang H, Ryman KD, Wang E, Fulop LD, Titball R, Barrett AD. 2004. Genetic relationships and evolution of genotypes of yellow fever virus and other members of the yellow fever virus group within the Flavivirus genus based on the 3' noncoding region. *J. Virol.* 78:9652–9665.
33. Proutski V, Gaunt MW, Gould EA, Holmes EC. 1997. Secondary structure of the 3'-untranslated region of yellow fever virus: implications for virulence, attenuation and vaccine development. *J. Gen. Virol.* 78(Pt 7):1543–1549.
34. Proutski V, Gould EA, Holmes EC. 1997. Secondary structure of the 3' untranslated region of flaviviruses: similarities and differences. *Nucleic Acids Res.* 25:1194 –1202.
35. Gritsun TS, Gould EA. 2006. Direct repeats in the 3' untranslated regions of mosquito-borne flaviviruses: possible implications for virus transmission. *J. Gen. Virol.* 87:3297–3305.
36. Bryant JE, Vasconcelos PF, Rijnbrand RC, Mutebi JP, Higgs S, Barrett AD. 2005. Size heterogeneity in the 3' noncoding region of South American isolates of yellow fever virus. *J. Virol.* 79:3807–3821.
37. Bae HG, Drosten C, Emmerich P, Colebunders R, Hantson P, Pest S, Parent M, Schmitz H, Warnat MA, Niedrig M. 2005. Analysis of two imported cases of yellow fever infection from Ivory Coast and The Gambia to Germany and Belgium. *J. Clin. Virol.* 33:274 –280.
38. Lefeuvre A, Contamin H, Decelle T, Fournier C, Lang J, Deubel V, Marianneau P. 2006. Host-cell interaction of attenuated and wild-type strains of yellow fever virus can be differentiated at early stages of hepatocyte infection. *Microbes Infect.* 8:1530 –1538.
39. Marianneau P, Megret F, Olivier R, Morens DM, Deubel V. 1996. Dengue 1 virus binding to human hepatoma HepG2 and simian Vero cell surfaces differs. *J. Gen. Virol.* 77(Pt 10):2547–2554.
40. Marianneau P, Steffan AM, Royer C, Drouet MT, Kirn A, Deubel V. 1998. Differing infection patterns of dengue and yellow fever viruses in a human hepatoma cell line. *J. Infect. Dis.* 178:1270 – 1278.
41. Thepparit C, Phoolcharoen W, Suksanpaisan L, Smith DR. 2004. Internalization and propagation of the dengue virus in human hepatoma (HepG2) cells. *Intervirology* 47:78–86.
42. Cooper LA, Scott TW. 2001. Differential evolution of eastern equine encephalitis virus populations in response to host cell type. *Genetics* 157:1403–1412.

## Tables and Figures

**Table 1.** Isolates of YFV analyzed in this study

Isolate no.	Accession no.	Isolate	Virus	Species	Yr	Location	Lineage	Source
333	JX898871	ArD 114896	YF	<i>Aedes aegypti</i> <sup>a</sup>	1995	Koungheul, Senegal	3	Institute Pasteur de Dakar, Senegal
335	JX898872	ArD 114972	YF	<i>Aedes aegypti</i> <sup>a</sup>	1995	Koungheul, Senegal	3	
357	JX898876	ArD 156468	YF	<i>Aedes furcifer</i>	2001	Kedougou, Senegal	4	
351	JX898875	ArD 149815	YF + Den2	<i>Aedes furcifer</i>	2000	Kedougou, Senegal	5	
345	JX898873	ArD 149214	YF	<i>Aedes furcifer</i>	2000	Kedougou, Senegal	5	
350	JX898874	ArD 149194	YF + Den2	<i>Aedes taylori</i>	2000	Kedougou, Senegal	5	
258	JX898868	HD 117294	YF	Human	1995	Koungheul, Senegal	6	
314	JX898870	ArD 121040	YF	<i>Aedes furcifer</i>	1996	Kedougou, Senegal	6	
307	JX898869	DakArAmt7	YF	<i>Aedes africanus</i>	1973	Côte d'Ivoire	1	
6857	JX898877	ArD 181464	YF	<i>Aedes furcifer</i>	2005	Kedougou, Senegal	4	
6858	JX898878	ArD 181250	YF	<i>Aedes furcifer</i>	2005	Kedougou, Senegal	4	
6865	JX898879	ArD 181676	YF	<i>Aedes taylori</i>	2005	Kedougou, Senegal	4	
6866	JX898880	ArD 181564	YF	<i>Aedes luteocephalus</i>	2005	Kedougou, Senegal	4	
6867	JX898881	ArD 181439	YF	<i>Aedes luteocephalus</i>	2005	Kedougou, Senegal	4	
		Asibi	YF	Human	1927	Ghana		Robert Koch Institute, Berlin, Germany
		17D RKI #142/94/1	YF	Human				

<sup>a</sup> Collected from male mosquitoes or female neonates.

**Table 2.** Sources of full genome sequences from GenBank used for phylogenetic analyses

Accession no.	YFV strain
AY640589.1	Asibi
AY603338.1	Strain isolated in Ivory Coast in 1999
AY572535.1	Strain isolated in Gambia in 2001
U21056.1	YFU21056 (French viscerotropic virus strain)
AF094612.1	Trinidad79A, 788379
U54798.1	YFU54798, 85-82H
DQ235229.1	Couma
AY968065.1	Uganda48a
AY968064.1	Angola71
JN620362	Uganda 2010
NC_008719	Sepik virus strain

**Table 3.** Amounts of amino acid differences of the various YFV lineages compared to Asibi over the whole coding region

Lineage	No. (%) of aa differences in the polyprotein compared to Asibi	No. (%) of unique features <sup>a</sup>	No. of unique features in protein:										
			C	prM	E	NS1	NS2A	NS2B	NS3	NS4A	2K	NS4B	NS5
Lineage 1	37 (1.08)	21 (56.8)	0	0	2	3	3	0	4	0	0	4	5
Lineage 3	30 (0.88)	27 (90.0)	2	2	6	0	2	1	2	1	1	4	6
Lineage 4 (strain 357)	23 (0.67)	5 (21.7)	0	0	3	0	0	0	1	0	0	0	1
Lineage 4 (2005)	27 (0.79)	6 (22.2)	0	0	2	0	0	2	0	0	0	1	1
Lineage 4 (total)	18 (0.53)	1 (5.5)	0	0	0	0	0	0	1	0	0	0	0
Lineage 5	29 (0.85)	5 (17.2)	2	0	0	1	0	1	0	0	0	1	0
Lineage 6	26 (0.76)	3 (11.5)	1	1	0	0	0	0	0	0	0	0	1

<sup>a</sup> Number of unique mutations that occur only in the indicated lineage. Percentages reflect the proportion of unique features for each lineage relative to the total number of aa differences from Asibi.

**Table 4.** Results of the immunofluorescence assay of Ap61 and HepG2 cells infected with the different YFV lineages within a time frame of 4 to 146 h postinfection (hpi)<sup>a</sup>

hpi	Percentage of Ap61 cells infected with strain:							Percentage of HepG2 cells infected with strain:						
	17D	Asibi	333	357	345	314	307	17D	Asibi	333	357	345	314	307
4	-	-	-	-	-	-	-	-	-	-	-	-	-	-
22	-	-	-	-	+	(-)	-	(+)	-	-	-	-	-	-
28	-	-	-	-	+(+)	(+)	(+)	(+)	-	(+)	(+)	(+)	(+)	(+)
50	(+)	-	-	+	++	+(+)	+(+)	+++(+)	+	++	+	+	-	+
75	-	(+)	-	++	++	+(+)	++	+++	+++	+++	+++(+)	+++	+++(+)	+++
99	(+)	+	-	+++(+)	++	++	+++(+)	+++	+++	+++	+++	+++	+++	+++
124	+	++	-	+++	+++	+++	+++	+++	+++	+++	+++	+++	+++	+++
146	+	++	-	+++	+++	+++	+++	+++	+++	+++	+++	+++	+++	+++

<sup>a</sup> Infection was visualized by fluorescence staining against the viral E protein, and results are given as percentages. Estimated percentages of infection are indicated as follows: (+), <10%; +, 10 to 40%; +( ), 40 to 50%; ++, 50 to 75%; +++(+), 75 to 85%; +++, 85 to 100%. A minus indicates no infection or a negative result.

**Figure 1.** Differences in the amino acid sequence throughout the viral polyprotein among the YFV strains that were completely sequenced in this study in comparison to the reference strain Asibi. Differences from the reference strain Asibi are highlighted in gray.

Protein:	C													prM			E													NS1			
	25	79	80	86	90	105	107	110	116	119	25	125	147	7	54	56	83	122	124	135	153	171	249	262	331	344	430	450	457	121	205	218	
Asibi	N	A	V	R	S	V	T	F	L	T	V	L	T	T	A	A	A	A	S	I	N	E	N	M	K	I	V	N	M	N	H	A	
L 1	307	N	A	V	R	S	V	T	F	L	T	V	L	T	T	A	A	A	A	S	I	N	E	N	M	K	V	I	S	M	N	H	T
L 3	333	N	A	A	R	G	V	T	F	L	T	M	F	T	A	V	A	A	A	S	I	K	E	D	M	R	I	V	N	I	N	H	A
	335	N	A	A	R	G	V	T	F	L	T	M	F	T	A	V	A	A	A	S	I	K	E	D	M	R	I	V	N	I	N	H	A
L 4	357	N	A	V	R	S	V	T	F	L	T	V	L	T	T	A	A/V	A	A	S	I	N	E	N	M	K	I	V	S	M	N	H	A
L 4 "2005"	6857	N	V	V	R	S	V	T	F	L	T	V	L	T	T	A	A	V	A	S	I/V	N	E	N	M	K	I	V	S	M	N	H	A
	6858	N	V	V	R	S	V	T	F	L	T	V	L	T	T	A	A	V	A	S	I/V	N	E	N	M	K	I	V	S	M	N	H	A
	6865	N	V	V	R	S	V	T	F	L	T	V	L	T	T	A	A	V	A	S	I/V	N	E	N	M	K	I	V	S	M	N	H	A
	6866	N	V	V	R	S	V	T	F	L	T	V	L	T	T	A	A	V	A	S	I/V	N	E	N	M	K	I	V	S	M	N	H	A
	6867	N	V	V	R	S	V	T	F	L	T	V	L	T	T	A	A	V	A	S	I/V	N	E	N	M	K	I	V	S	M	N	H	A
L 5	345	N	A	V	R	S	A	T	L	I	A	V	L	T	T	A	A	A	A	S	I	N	E	N	T	K	I	V	S	M	S	H	A
	350	N	A	V	R	S	A	T	L	I	A	V	L	T	T	A	A	A	A	S	I	N	E	N	M	K	I	V	S	M	S	H	A
	351	N	A	V	R	S	A	T	L	I	A	V	L	T	T	A	A	A	A	S	I	N	K	N	M	K	I	V	S	M	S	H	A
L 6	258	N	A	V	R	S	A	F	L	A	V	L	M	T	A	A	A	A	A	S	I	N	E	N	M	K	I	V	S	M	N	H	A
	314	S	V	V	K	S	A	A	F	L	A	V	L	M	T	A	A	A	A	S	I	N	E	N	M	K	I	V	S	M	N	N	A

Protein:	NS1			NS2A							NS2B							NS3															
	240	276	326	3	35	55	82	105	147	189	220	9	45	47	54	60	79	126	13	89	111	192	253	254	280	347	397	444	515	535	545	594	
Asibi	E	K	S	I	V	T	I	T	T	Q	I	A	A	R	K	S	S	R	I	G	V	M	S	A	V	E	R	K	V	K	D	K	
L 1	307	D	K	N	V	M	T	I	T	V	Q	I	A	A	R	K	S	S	R	I	G	V	M	S	A	I	E	K	K	I	R	D	K
L 3	333	E	K	S	I	V	T	V	A	T	Q	I	A	A	R	K	A	S	R	V	G	V	K	S	A	I	E	R	K	V	K	D	K
	335	E	K	S	I	V	T	V	A	T	Q	I	A	A	R	K	A	S	R	V	G	V	K	S	A	I	E	R	K	V	K	D	K
L 4	357	E	R	S	I	V	T	I	T	T	Q	L	A	A	R	R	S	S	K	I	G	I	M	S	A	I	E	R	K	V	K	D	K
L 4 "2005"	6857	E	R	S	I	V	I	I	T	T	Q	L	T	V	R	R	S	S	K	I	G	I	M	S	A	I	E	R	K	V	K	D	K
	6858	E	R	S	I	V	I	I	T	T	Q	L	T	V	R	R	S	S	K	I	G	I	M	S	A	I	E	R	K	V	K	D	K
	6865	E	R	S	I	V	I	I	T	T	Q	L	T	V	R	R	S	S	K	I	G	I	M	S	A	I	E	R	K	V	K	D	K
	6866	E	R	S	I	V	I	I	T	T	Q	L	T	V	R	R	S	S	K	I	G	I	M	S	A	I	E	R	K	V	K	D	K
	6867	E	R	S	I	V	I	I	T	T	Q	L	T	V	R	R	S	S	K	I	G	I	M	S	A	I	E	R	K	V	K	D	K
L 5	345	E	R	S	I	V	I	I	T	T	Q	L	A	A	R	R	S	N	K	I	G	V	M	S	A	I	E	R	K	V	K	G	K
	350	E	R	S	I	V	I	I	T	T	Q	L	A	A	R	R	S	N	K	I	G	V	M	S	A	I	E	R	K	V	K	D	K
	351	E	R	S	I	V	I	I	T	T	Q	L	A	A	G	R	S	N	K	I	G	V	M	S	A	I	E	R	V	K	D	K	
L 6	258	E	R	S	I	V	T	I	T	T	Q	L	A	A	R	R	S	S	K	I	S	V	M	S	G	I	G	R	K	V	K	D	K
	314	E	R	S	I	V	T	I	T	T	R	L	A	A	R	R	S	S	K	I	G	V	M	S	A	I	E	R	K	V	K	D	K

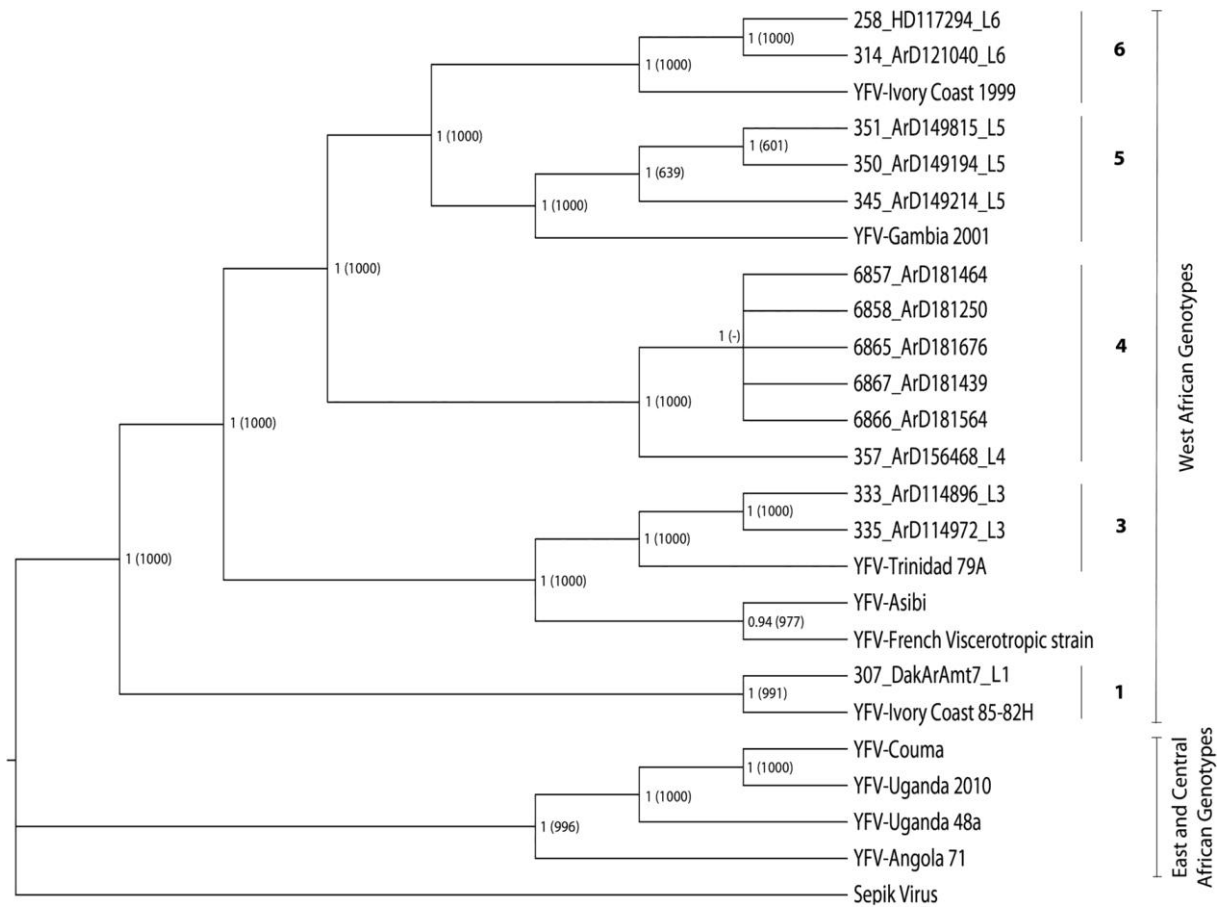
  

Protein:	NS3		NS4A		2K		NS4B											NS5															
	613	614	30	9	8	16	18	19	32	95	98	117	121	145	165	182	246	2	78	108	138	162	245	258	275	292	295	335	531	594	641	643	
Asibi	S	E	F	Y	K	K	N	L	L	I	V	M	S	E	A	A	K	S	I	D	V	V	R	I	K	S	Y	R	F	V	E	V	
L 1	307	A	D	F	Y	R	R	N	L	L	I	V	M	T	K	A	A	E	R	T	E	V	V	R	I	R	T	Y	R	F	V	D	A
L 3	333	S	E	L	F	K	K	N	S	F	M	I	M	S	K	V	A	K	T	I	D	V	V	R	T	K	S	Y	K	L	V	E	V
	335	S	E	L	F	K	K	N	S	F	M	I	M	S	K	V	A	K	T	I	D	V	V	R	T	K	S	Y	K	L	V	E	V
L 4 "2005"	357	A	D	F	Y	K	K	N	L	L	I	V	M	S	K	A	A	K	S	T	D	V	M	R	I	R	T	Y	R	F	V	E	A
	6857	A	D	F	Y	K	K	N	L	L	I	V	M	S	K	A	A	N	R	T	D	V	M	R	I	R	T	Y	R	F	I	E	A
	6858	A	D	F	Y	K	K	N	L	L	I	V	M	S	K	A	A	N	R	T	D	V	M	R	I	R	T	Y	R	F	I	E	A
	6865	A	D	F	Y	K	K	N	L	L	I	V	M	S	K	A	A	N	R	T	D	V	M	R	I	R	T	Y	R	F	I	E	A
	6866	A	D	F	Y	K	K	N	L	L	I	V	M	S	K	A	A	N	R	T	D	V	M	R	I	R	T	Y	R	F	I	E	A
L 5	345	A	D	F	Y	K	K	D	L	L	I	V	T	S	K	A	S	K	R	T	D	V	M	R	I	R	T	Y	R	F	V	E	A
	350	A	D	F	Y	K	K	D	L	L	I	V	T	S	K	A	S	K	R	T	D	V	M	G	I	R	T	Y	R	F	V	E	A
	351	A	D	F	Y	K	K	D	L	L	I	V	T	S	K	A	S	K	R	T	D	V	M	R	I	R	T	Y	R	F	V	E	A
L 6	258	A	D	F	Y	K	K	D	S	L	I	V	T	S	K	A	A	K	R	T	D	M	M	R	I	R	T	H	R	F	V	E	A
	314	A	D	F	Y	K	K	D	S	L	I	V	T	S	K	A	A	K	R	T	D	M	M	R	I	R	T	Y	R	F	V	E	A

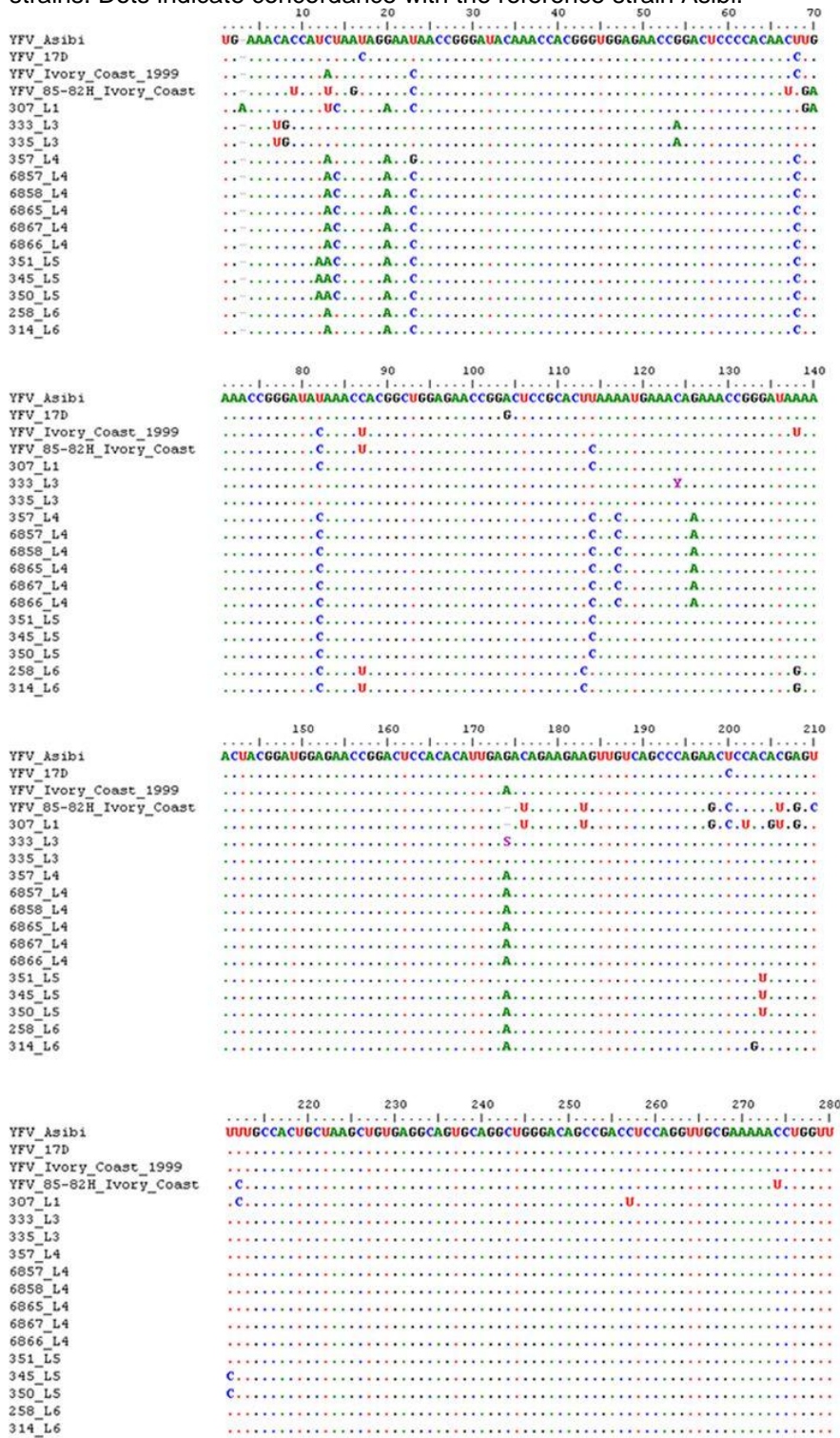
  

Protein:	NS5										
	645	652	657	660	680	810	815	833	878	882	
Asibi	T	T	N	K	L	T	E	M	I	K	
L 1	307	A	I	D	K	M	P	E	V	I	K
L 3	333	T	T	N	R	L	T	E	M	V	K
	335	T	T	N	R	L	T	E	M	V	K
L 4	357	T	T	D	K	L	T	G	V	I	R
L 4 "2005"	6857	T	T	D	K	L	T	G	V	I	K
	6858	T	T	D	K	L	T	G	V	I	K
	6865	T	T	D	K	L	T	G	V	I	K
	6866	T	T	D	K	L	T	G	V	I	K
	6867	T	T	D	K	L	T	G	V	I	K
L 5	345	A	T	D	K	L	T	G	V	I	K
	350	A	T	D	K	L	T	G	V	I	K
	351	A	T	D	K	L	T	G	V	I	K
L 6	258	T	T	D	K	L	T	G	V	I	K
	314	T	T	D	K	L	T	G	V	I	K

**Figure 2.** Majority rule consensus tree of the Bayesian analysis, with 10 million generations based on YFV full genome sequences. Posterior probability values are displayed beside the related node. Bootstrap values of the ML analysis are given in parentheses. Note that unsupported values of 50/0.5 or less are indicated by a minus sign. The appropriate lineages of the already classified YF strains are specified at the end of the labels as L1 to L6.



**Figure 3.** RNA sequence alignment of the 3'-nontranslated region (3'-NTR) of 18 West African YFV strains. Dots indicate concordance with the reference strain Asibi.



```

                290      300      310      320      330      340      350
.....|.....|.....|.....|.....|.....|.....|.....|
YFV_Asibi      UCUGGGACUCCACCCAGAGU AAAAAAGACGGAGCCUCCGCUACCACCUCCACCGUGGUGAGAA
YFV_17D
YFV_Ivory_Coast_1999
YFV_85-82H_Ivory_Coast
307_L1
333_L3
335_L3
357_L4
6857_L4
6858_L4
6865_L4
6867_L4
6866_L4
351_LS
345_LS
350_LS
258_L6
314_L6

```

```

                360      370      380      390      400      410      420
.....|.....|.....|.....|.....|.....|.....|
YFV_Asibi      AGACGGGGUCUAGAGGUUAGAGGAGACCCUCCAGGGAAACAAUAGUGGGACCAUUAUGACGCCAGGGAAA
YFV_17D
YFV_Ivory_Coast_1999
YFV_85-82H_Ivory_Coast
307_L1
333_L3
335_L3
357_L4
6857_L4
6858_L4
6865_L4
6867_L4
6866_L4
351_LS
345_LS
350_LS
258_L6
314_L6

```

```

                430      440      450      460      470      480      490
.....|.....|.....|.....|.....|.....|.....|
YFV_Asibi      GACCGGAGUGGUUCUGGCUUUUCCUCCAGGGGUCUGUGAGCACAGUUUUGCUCAGAAUAAGCAGACCUU
YFV_17D
YFV_Ivory_Coast_1999
YFV_85-82H_Ivory_Coast
307_L1
333_L3
335_L3
357_L4
6857_L4
6858_L4
6865_L4
6867_L4
6866_L4
351_LS
345_LS
350_LS
258_L6
314_L6

```

```

                500      510
.....|.....|.....|
YFV_Asibi      UGGAGAAAAACAAAAACACU
YFV_17D
YFV_Ivory_Coast_1999
YFV_85-82H_Ivory_Coast
307_L1
333_L3
335_L3
357_L4
6857_L4
6858_L4
6865_L4
6867_L4
6866_L4
351_LS
345_LS
350_LS
258_L6
314_L6

```

**Figure 4.** Growth kinetics of the strains Asibi (a), 357 (lineage 4) (b), and 333 (lineage 3) (c). The diagrams show the amount of viral RNA equivalents isolated from supernatants (●) and cells (■) (genome equivalents [GE]/ml), as well as the number of infectious viral particles (▲) (PFU/ml) over a time period of 146 h postinfection. The experiments were performed with Ap61 cells (dotted lines) and HepG2 cells (continuous lines). Range values of two independent experiments are indicated by the error bars in the lines reflecting RNA equivalents isolated from supernatants.

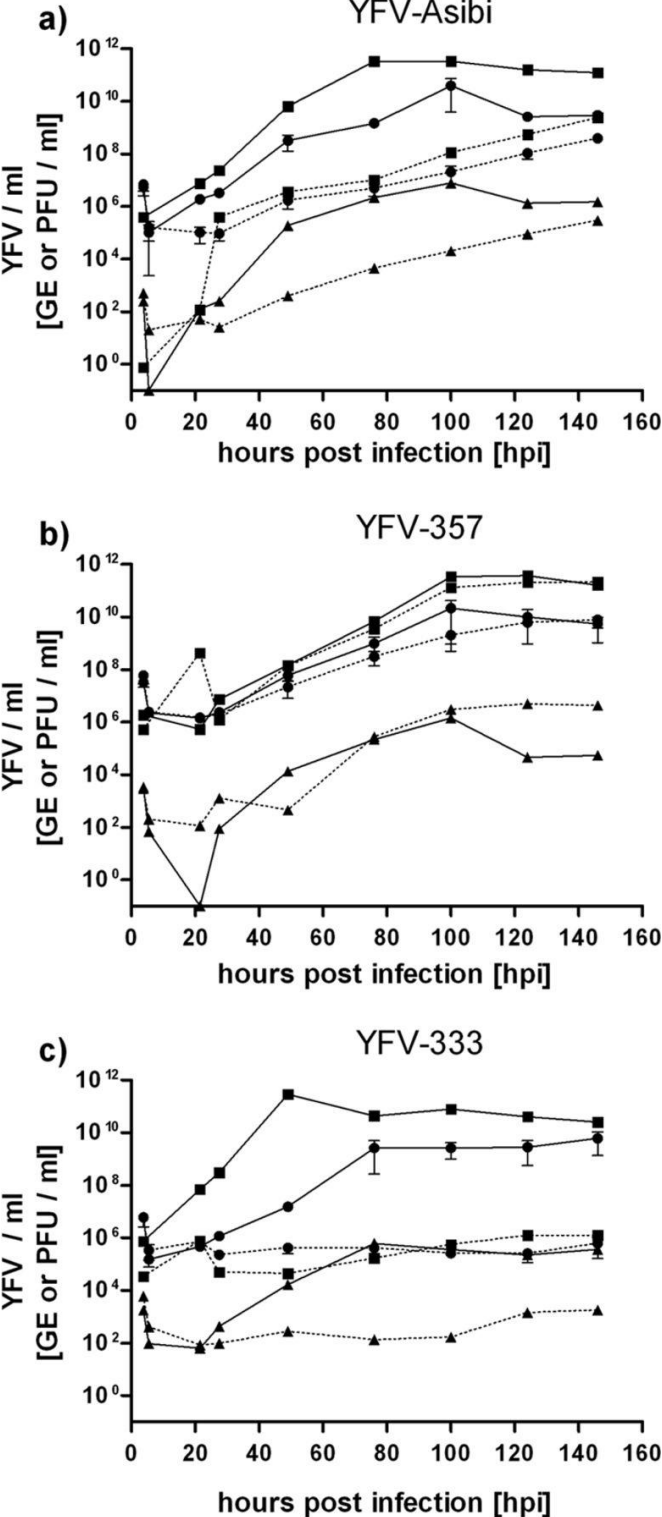


**Figure 5.** Immunofluorescence assay of Ap61 and HepG2 cells infected with YFV Asibi or YFV 357 within a time period of 50 to 146 h postinfection. Staining occurred against the viral E protein (MAK6330) and the nucleus (DAPI) as described above.

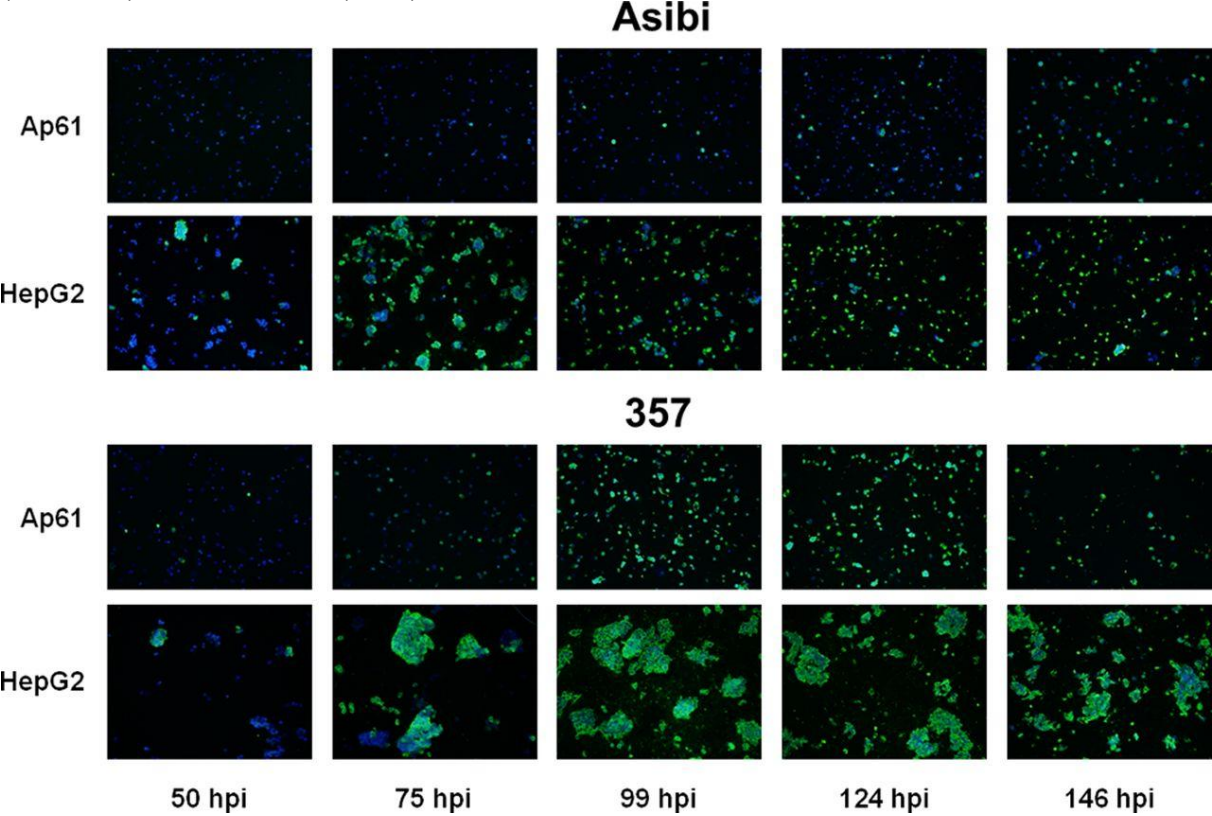


**Figure 6.** Growth curves of the different YF lineages in HepG2 cells. Analyzed parameters are the quantity of viral RNA copies isolated from cell culture supernatants (a) and from cells directly (b) (GE/ml) and the quantity of infectious viral particles (c) (PFU/ml). Range values of two independent experiments are indicated by the error bars in panel a.

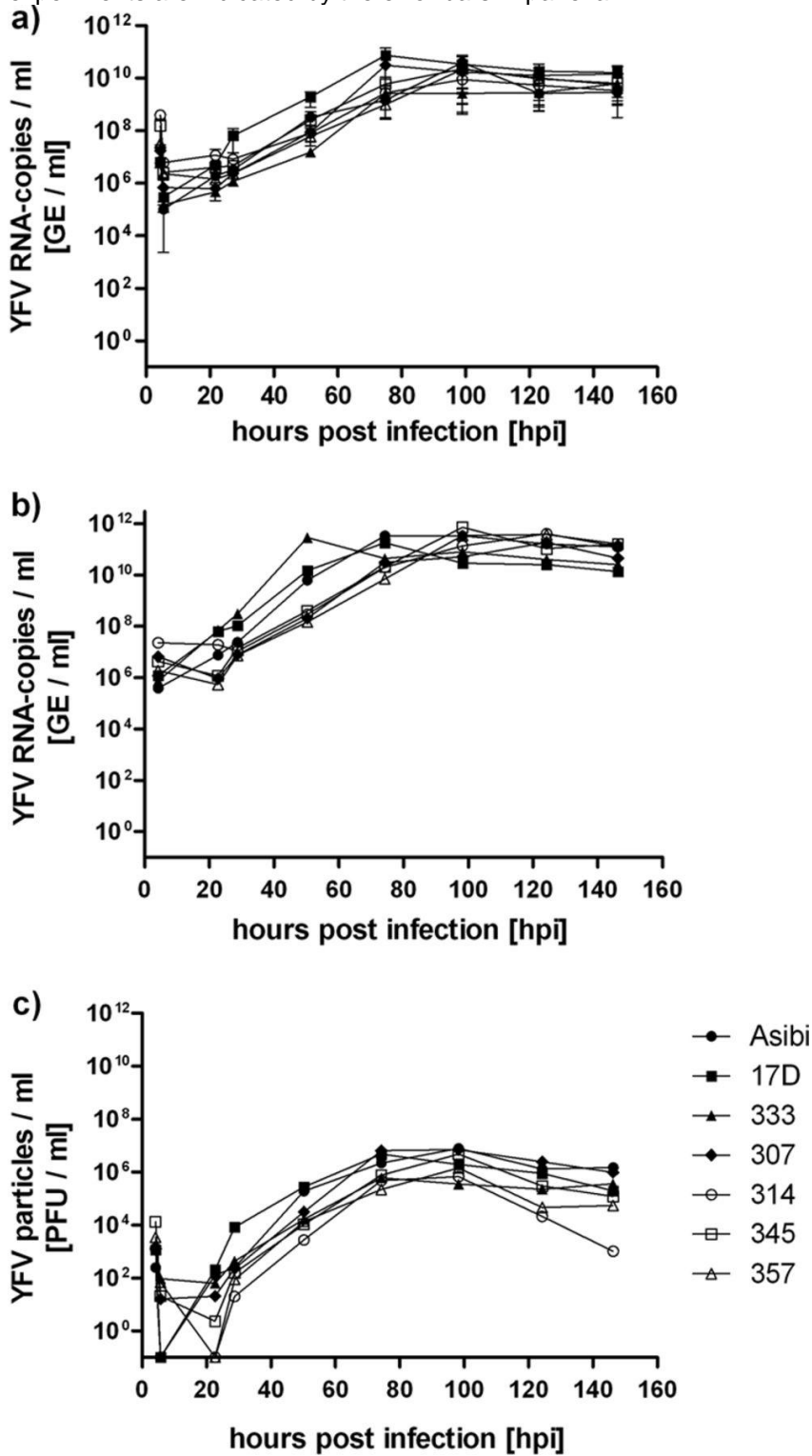


**Figure 7.** Growth curves of all tested strains determined with Ap61 cells. Analyzed parameters are the quantity of viral RNA copies isolated from cell culture supernatants (a) and from cells (b) (GE/ml) and the quantity of infectious viral particles (c) (PFU/ml). Range values of two independent experiments are indicated by the error bars in panel a.

